Isorhamnetin inhibits progression of ovarian cancer by targeting ESR1

Manman Wang, Zhengtan Xu, Qi Cai, Yanmei Deng, Weiqiao Shi, Hongyu Zhou, Dajiang Wang, Jian Li

Department of Pharmacy, West China Hospital of Sichuan University, Chengdu, China

Contributions: (I) Conception and design: All authors; (II) Administrative support: J Li; (III) Provision of study materials or patients: M Wang, Z Xu, Q Cai; (IV) Collection and assembly of data: M Wang, W Shi, H Zhou; (V) Data analysis and interpretation: All authors; (VI) Manuscript writing: All authors; (VII) Final approval of manuscript: All authors.

Correspondence to: Jian Li. Department of Pharmacy, West China Hospital of Sichuan University, Chengdu 610041, China. Email: jianli67@163.com.

Background: Although reports suggest Chinese herbal medicine treatment of ovarian cancer (OC) has a good effect, the role of isorhamnetin (ISO), a flavonol aglycone with immune, anti-inflammatory, cardiovascular and cerebrovascular protective effects, as well as an anticancer effect, in OC remains unclear. Network pharmacology was used to explore this *in vitro* and *in vivo*, and to identify relevant targets.

Methods: The common targets of ISO in the treatment of OC were screened by constructing drug targets and disease gene databases for Gene Ontology (GO) and Kyoto Encyclopedia of Genes and Genomes (KEGG) enrichment analyses. The protein-protein interaction network was constructed by STRING. Overlapping targets were further analyzed using the online tool UALCAN to analyze the correlation between gene expression and patient survival and prognosis. The effect of ISO on OC cell proliferation, migration, and invasion was assessed *in vivo* and *in vitro*, and the function of the estrogen receptor 1 (ESR1) in the development of OC was examined by overexpressing and knocking down *ESR1* expression.

Results: Through network pharmacology analysis, 25 target genes related to ISO-OC were screened out. The overall survival rate of OC patients only significantly correlated with high expression of *ESR1* among 13 highly expressed overlapping genes. ISO significantly inhibited the proliferation, migration and invasion of OC cells *in vitro* and inhibited tumor growth *in vivo*. Overexpression of *ESR1* significantly promoted the proliferation, migration and invasion of OC cells, whereas knockdown of *ESR1* showed the opposite result. In addition, overexpression of *ESR1* significantly reversed the inhibitory effect of ISO on the proliferation, migration and invasion of OC cells.

Conclusions: We confirmed that ISO inhibits OC cell proliferation, migration and invasion by targeting *ESR1* expression, which provides a theoretical basis for further pharmacological research.

Keywords: Estrogen receptor 1 (ESR1); isorhamnetin (ISO); network pharmacology; ovarian cancer (OC); proliferation

Introduction

Ovarian cancer (OC) is characterized by hidden onset, lack of early clinical symptoms, and high recurrence rate. It is the gynecological malignant tumor with the highest mortality rate (1). At present, the treatment of OC is mainly based on surgery and postoperative combined chemotherapy, immunotherapy and radiotherapy (2). However, due to the weakness of patients and the adverse reactions of chemotherapy, the outcome of western medical treatment is often affected, so new strategies are needed to reduce the progression and mortality of OC.

In recent years, natural-derived components have attracted much attention due to their potential

Page 2 of 13

Wang et al. Study on the anti-tumor effect of ISO in OC

tumor selectivity, cytotoxic effects and few side effects. Isorhamnetin (ISO) (3'-methoxy-3,4',5,7-tetrahydroxyflavone), a flavonol aglycone, which is rich in fruits, vegetables and tea, as well as traditional medicines such as *Hippophae rhamnoides* (L.), *Vernonia anthelmintica* (L.), and *Astragalus membranaceus* (Fisch.) (3,4). A variety of studies have shown that ISO has a significant role in immune regulation, anti-inflammatory, cardiovascular and cerebrovascular protection (5-7). In addition, its anticancer effect has been confirmed in colon cancer (8), breast cancer (9) and lung cancer (10). In these tumors, ISO exhibits comprehensive antitumor activity by inhibiting cell proliferation and migration and activating apoptosis (10,11). Although the inhibitory effect of ISO on cancer cells has been widely studied, its potential role and molecular mechanism in OC treatment are still unclear.

Network pharmacology is a valuable new method that integrates system biology and bioinformatics to elucidate the complex mechanisms of drugs (12). It has been applied to predict protein targets and disease pathways of natural plant components (13). In this study, the target of ISO for OC was predicted based on a public database, and then a protein-protein interaction (PPI) network was created and Gene Ontology (GO) and Kyoto Encyclopedia of Genes and Genomes (KEGG) pathway enrichment analyses were performed. Finally, we conducted *in vitro* and *in vivo* experiments to verify the results. We present the following article in accordance with the ARRIVE reporting checklist (available at https://atm.amegroups.com/article/view/10.21037/atm-22-5064/rc).

Methods

Prediction of ISO targets and identification of OC-related genes

The 3D molecular structure (SDF format) of ISO was downloaded from the PubChem database (https://pubchem.ncbi.nlm.nih.gov/), then uploaded SDF files to PharmMapper (http://www.lilab-ecust.cn/pharmmapper/) to predict drug targets. OC-related targets were obtained from the GeneCard database (https://www.genecards.org/). The intersection of ISO and OC target genes was drawn by Venn diagram (https://biiofogp.cnb.csic.es/tools/venny/) with VENNY 2.1. In the plotting operation, 114 ISO target genes and 625 OC-related targets were input, and 25 cross-targets were obtained.

GO and KEGG analyses

GO and KEGG enrichment analyses were performed using the Metascape database (http://metascape.org/gp/index.html#/main/step1) to further explore the potential biological functions and mechanisms of the target genes. The GO and KEGG analysis results are shown as bar charts and bubble charts, respectively.

Construction of PPI network

The overlapping genes were imported into the STRING database (https://string-db.org/) to construct the PPI network, and then visualized by Cytoscape 3.8.2 software.

Differential expression analysis of overlapping genes

Based on GEO2R (http://www.ncbi.nlm.nih.gov/geo/geo2r/) analysis of the GSE66957 database, with |Log2[fold change (FC)]| >1 and corrected P value <0.01 as the truncation standard, the differentially expressed upregulated genes were obtained and intersected with the above 25 target genes, from which 13 common genes were found.

Overlapping gene expression and survival analysis of OC patients

Cancer transcriptome data from clinical patients were analyzed using the online public cancer transcriptome database UALCAN (http://ualcan.path.uab.edu/), which can compare and analyze the expression of a gene in normal and tumor samples, and evaluate the effect of clinicopathological features and gene expression levels on patient survival (14). Subsequently, Kaplan-Meier (K-M) survival analysis was performed on the target genes to explore the value and significance of each single gene in OC prognostic prediction.

Cell culture and transfection

Human OC cell lines (SKOV-3 and HO8910) were purchased from the American Type Culture Collection (ATCC, USA). The cells were cultured in RPMI-1640 medium (Gibco, USA) containing 10% fetal bovine serum (FBS; Gibco, USA) and 1% penicillin/streptomycin (100×) (Yeasen, Shanghai, China) at 37 ℃ in a 5% CO_2 incubator, before being seeded in 12-well plates at a density

of 1×10^6 cells/well. When the cell confluence reached 80%, Lipofectamine 2000 (Invitrogen, USA) and serum-free RPMI-1640 medium (Gibco, USA) were used for transfection. After 6 h of transfection, the culture medium was updated to fresh medium, cell cultivation continued, and follow-up experiments were performed after 24 h. Estrogen receptor 1 (ESR1) overexpression plasmid and its negative control empty vector (Vector), shRNA-ESR11# (shESR1 1#), shESR1 2# and its negative control shNC were all obtained from GenePharma Ltd., Co. (Shanghai, China).

Cell Counting Kit 8 (CCK8) assay

SKOV3 and HO8910 cells were seeded in 96-well plates at 100 µL/well ($\approx1\times10^4$) and cultured in a 5% CO_2 incubator at 37 ℃ for 24 h. After treatment with 0, 5, 10, 15 or 20 µM ISO (Sigma-Aldrich, USA), ISO concentration setting based on research by Hu *et al.* (6) or the corresponding transfection treatment according to the experimental protocol, 10 µL CCK-8 solution (Beyotime, Shanghai, China) was added to each well, and cultured at 37 ℃ for 2 h. The absorbance at 450 nm was detected by a microplate reader (Bio-Tek, USA).

Colony formation experiment

SKOV3 and HO8910 cells were cultured overnight in 6-well plates (500 cells/well) and then treated with 15 µM ISO or vector for 24 h. After treatment, the cells were cultured in complete medium for 15 days and the medium was replaced every 2 days. Cell colonies were fixed with 4% paraformaldehyde (PFA) and stained with 1% crystal violet staining solution. The number of colonies >50 cells was counted under an optical microscope (Olympus, Japan).

Wound healing test

SKOV3 and HO8910 cells were seeded in 6-well plates at a density of 2×10^5 cells/well and cultured to about 100% confluence. Scratches were generated by scraping monolayer cells with a 200-µL pipette tip, and then washed three times with serum-free medium to remove unattached cells. The wounds were then treated with 15 µM ISO or vector for 24 h. Wound areas were photographed under a microscope (Olympus, Japan) for 0 and 24 h, and wound closure was quantified using ImageJ software.

Transwell assay

SKOV3 and HO8910 cells were seeded in serum-free medium, with 15 µM ISO or vector added, then seeded in the upper chamber of a Matrigel-coated transwell chamber (Corning, Cambridge, USA); 600 µL RPMI-1640 medium (5% FBS) was added to the lower chamber. After 24 h incubation, the non-migrating cells on the upper surface of the membrane were removed with a cotton swab, and the cells penetrating the lower surface of the membrane were stained with crystal violet. Cells were counted from five random microscopic fields using ImageJ software.

Western blotting

The total proteins were extracted from SKOV3 and HO8910 cells and quantified by BCA protein analysis kit (Beyotime), then separated by sodium dodecyl sulfate-polyacrylamide gel electrophoresis (SDS-PAGE). After separation, each protein was transferred to a polyvinylidene fluoride (PVDF) membrane (Millipore, USA), which was blocked with 5% skimmed milk at room temperature for 2 h and then incubated with the corresponding primary antibody overnight at 4 ℃. The membrane was washed three times with phosphate buffer solution with 0.1% Tween-20 (PBST) for 10 min each time, and incubated with secondary antibody at 37 ℃ for 1 h. Protein bands were visualized using an imaging system and enhanced chemiluminescence (ECL) reagents (Millipore, USA). β-actin was used as an internal control, and the results were analyzed using ImageJ software. The primary antibodies used were: β-actin (1:500, ab115777, Abcam), Ki67 (1:1,000, ab16667, Abcam), matrix metalloproteinase (MMP)9 (1:1,000, ab228402, Abcam), MMP2 (1:1,000, ab92536, Abcam), and ESR1 (1:1,000, ab108398, Abcam).

Tumor xenograft model

For the *in vivo* experiment, 5-week-old female BALB/c nude mice (18–20 g bodyweight) were purchased from Beijing Vital River Laboratory Animal Technology Co., Ltd., and raised under standard laboratory conditions. The light and dark cycle was 12 h. A tumor xenograft model was established by subcutaneous injection of SKOV3 cells into the under the skin of the righthand side of the abdomen of mice (100 µL, 2×10^7 cells). On the 7th day after injection of SKOV3 cells, the mice were randomly divided into a

Page 4 of 13

Wang et al. Study on the anti-tumor effect of ISO in OC

control group and ISO group (20 mg/kg, 5 mice in each group). The ISO group was treated with 20 mg/kg ISO (6), and the control group was treated with an equal volume of dimethyl sulfoxide (DMSO; Sigma-Aldrich, USA), by intravenous injection once every other day. The first day of ISO treatment was defined as day 1. The length (L) and width (W) of the tumor were measured every other day; tumor volume (V) = (L × W^2)/2 (15). At the end of the treatment, the mice were executed by decortication, the tumors were removed, weighed, the tumor size was measured and the volume was calculated. Animal experiments were performed under a project license (No. 20221014004) granted by ethics committee of West China Hospital of Sichuan University, in compliance with national guidelines for the care and use of animals. A protocol was prepared before the study without registration.

Statistical analysis

The results are expressed as mean ± standard deviation (SD), and data analysis was performed using SPSS 23.0 a and GraphPad Prism (Version 8.0). The relationship between ERS1 expression and overall survival (OS) of OC patients was analyzed by K-M survival curve and log-rank analysis. One-way ANOVA and Student's t-test were used to analyze the results. A level of $P<0.05$ was deemed significant.

Results

Screening and functional analysis of target genes of ISO in treatment of OC

We used the PharmMapper platform to predict the potential binding genes of ISO. Finally, 114 genes were predicted to be ISO binding genes, and 625 OC-related genes were obtained from the GeneCard database. Using Venny 2.1.0 mapping software, ISO-regulated targets were intersected with OC targets to obtain 25 intersectional genes (*Figure 1A*). In order to elucidate the potential mechanism of ISO on OC regulation, we used Metascape software to analyze the GO and KEGG pathways of the 25 intersection genes. As shown in *Figure 1B*, GO enrichment analysis includes biological processes (BP), cellular components (CC), and molecular functions (MF). We found that BP was related to cell apoptosis, proliferation, migration and drug response, etc., CC was related to receptor complexes, mitochondria, endoplasmic reticulum membrane, etc., and MF were related to organic cyclic compound binding, drug

binding and kinase activity, etc. KEGG analysis showed that overlapping gene enriched the PI3K-Akt signaling pathway, MAPK signaling pathway, and Ras signaling pathway, which may be the potential pharmacological mechanisms of ISO in the treatment of OC (*Figure 1C*). In order to explore the protein interactions among the 25 overlapping targets of ISO and OC, the gene information was uploaded to the STRING database to form a PPI network diagram (*Figure 1D*).

Expression and survival analysis of target genes of ISO and OC intersection

We used the GEO2R tool to screen 7,684 upregulated genes from the GSE66957 database that intersected with the 25 genes by Venny 2.1.0 mapping software, and found 13 overlapping genes (*Figure 2A,2B*). As shown in *Figure 2C*, we found that the expression of ESR1 mRNA in OC samples was significantly higher than that in normal controls (P<0.01). In order to further clarify the prognostic value of these overlapping genes, we analyzed the OS of OC patients through the UALCAN database and K-M plotter. As shown in *Figure 2D*, we found that high expression of ESR1 mRNA was associated with low OS (P<0.05); other genes had no statistical effect on OS. Compared with the good prognosis group, the expression of ESR1 in the poor prognosis group was significantly upregulated (P<0.05, *Figure 2E*). Notably, patients with high ESR1 expression had significantly shorter disease-free survival than patients with low ESR1 expression (P<0.05, *Figure 2F*).

Effect of ISO on the proliferation, migration and invasion of OC cells

The cytotoxicity of 5, 10, 15 and 20 µM ISO on human OC cells (SKOV3 and HO8910) was determined by CCK-8 assay. ISO significantly decreased the viability of SKOV3 and HO8910 cells in a dose-dependent manner compared with 0 µM ISO (Control) group (P<0.05). When the concentration was 15 µM, ISO reduced the viability of SKOV3 and HO8910 cells to ≈53% and 50%, respectively (*Figure 3A,3B*). Therefore, 15 µM ISO was selected as the treatment dose in subsequent experiments. As shown in *Figure 3C-3H*, we found that 15 µM ISO inhibited the cell viability of SKOV3 and HO8910 in a time-dependent manner, and significantly inhibited cell colony formation, wound healing and invasion (P<0.05). In addition, Western blot was used to detect the protein levels of proliferation and invasion-related biomarkers after ISO treatment. The
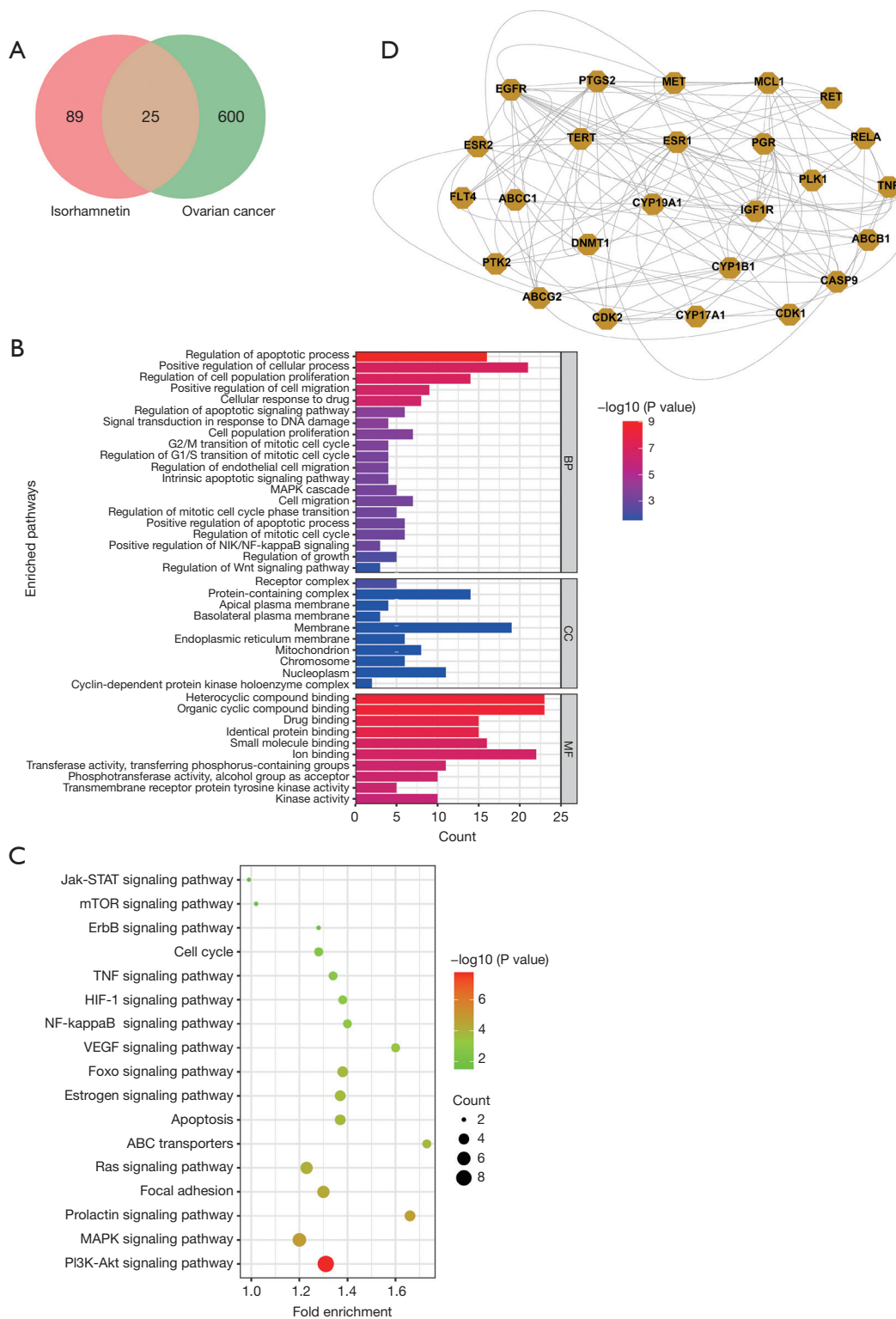
Figure 1 Target screening and functional analysis of ISO in OC. (A) Venn diagram shows 25 intersectional target genes of 114 ISO target genes and 625 OC target genes. (B) GO functional enrichment analysis. (C) KEGG enrichment analysis. (D) PPI network analysis. ISO, isorhamnetin; OC, ovarian cancer; GO, Gene Ontology; KEGG, Kyoto Encyclopedia of Genes and Genomes; PPI, protein-protein interaction; BP, biological processes; CC, cellular components; MF, molecular functions; ABC, ATP-binding cassette.
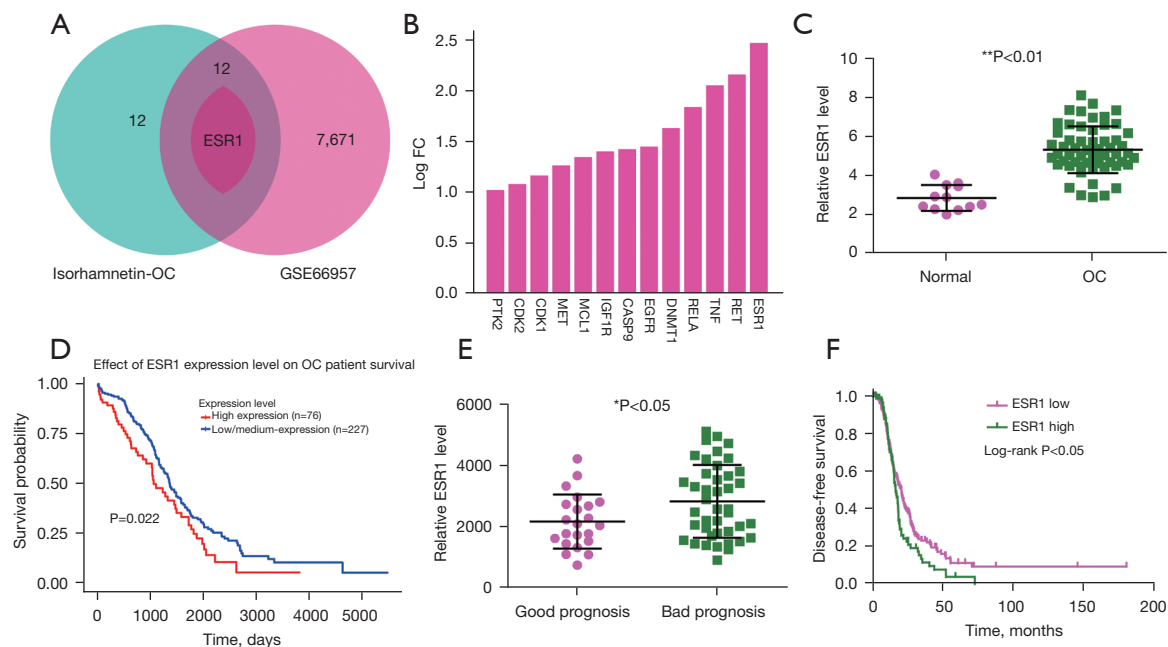
Page 6 of 13

Wang et al. Study on the anti-tumor effect of ISO in OC

Figure 2 Survival analysis identification of ISO therapeutic OC targets. (A) Venn diagram shows the upregulated genes in the GSE66957 database and 13 overlapping genes among 25 intersection target genes. (B) mRNA expression levels of the 13 overlapping genes. (C) Expression of ESR1 in OC and normal tissues. (D) Analysis of ESR1 expression and overall survival in patients with OC. (E) Expression of ESR1 in patients with good and poor prognoses. (F) Analysis of ESR1 expression and disease-free survival in patients with OC. Comparison with corresponding group, *, $P<0.05$; **, $P<0.01$. ISO, isorhamnetin; OC, ovarian cancer; ESR1, estrogen receptor 1; FC, fold change.

results showed that the protein levels of Ki67, MMP9, and MMP2 in SKOV3 and HO8910 cells were significantly decreased after 15 µM ISO treatment ($P<0.05$, *Figure 3I*), which suggested that the anti-metastatic effect of ISO on OC cells is related to inhibition of MMP2 and MMP9 protein expression.

Effect of ISO on tumor growth of OC *in vivo*

A xenograft mouse model was established to explore the antitumor effect of ISO *in vivo*. As shown in *Figure 4*, compared with the Control group, the tumor volume and weight of the ISO (20 mg/kg) group were significantly reduced ($P<0.05$), which indicated that ISO inhibited the growth of OC cell xenografts in nude mice.

Effect of ESR1 on the proliferation, migration and invasion of OC cells *in vitro*

The role of ESR1 in the proliferation, migration and invasion of OC cells was detected by overexpression or knockdown of ESR1 expression. The protein levels of ESR1 in SKOV3 and HO8910 cells transfected with

vector, ESR1were detected by western blotting. The results showed that, in SKOV3 and HO8910 cells, the level of ESR1 protein in ESR1 group was significantly increased (*Figure 5A*). Subsequently, as shown in *Figure 5B-5G*, CCK-8, colony formation, wound healing and transwell analysis showed that the viability of SKOV3 and HO8910 cells was enhanced, and the numbers of colonies and invasive cells increased significantly, while the wound width decreased significantly at 24 h after overexpression of ESR1 ($P<0.05$), indicating that ESR1 overexpression promoted the proliferation, migration and invasion of OC cells. Western blotting experiment showed that, in SKOV3 and HO8910 cells, the level of ESR1 protein in the shESR1 1# and shESR1 2# groups were significantly decreased than in the shNC group (*Figure 5H*). And knockdown of ESR1 expression inhibited the proliferation, migration and invasion of OC cells (*Figure 5I-5N*).

Effect of ISO on the proliferation, migration and invasion of OC cells mediated by ESR1

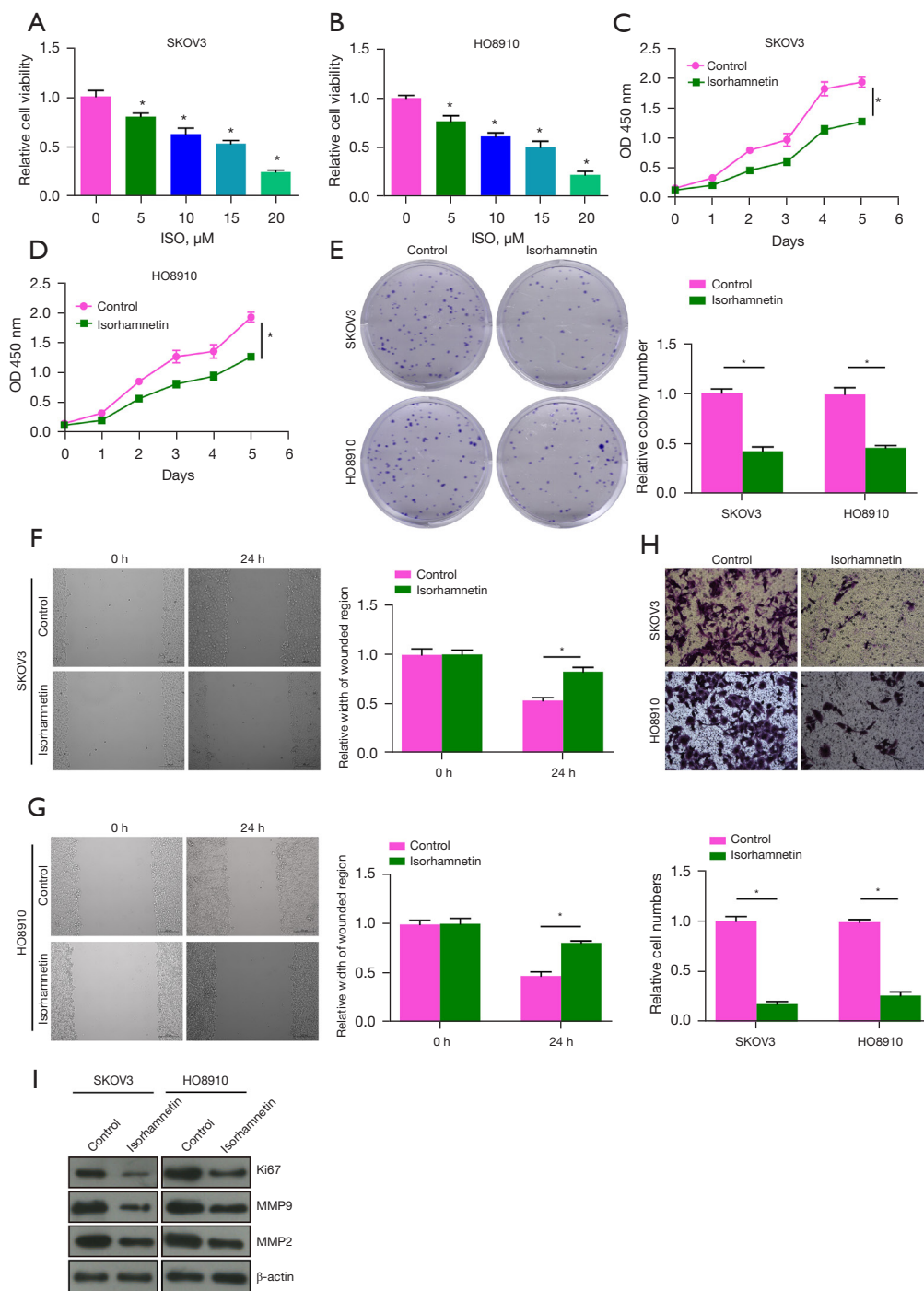The protein levels of ESR1 in SKOV3 and HO8910 cells treated with 5, 10, 15 and 20 µM ISO for 24 h were detected

Figure 3 ISO inhibits the proliferation, migration and invasion of SKOV3 and HO8910 cells *in vitro*. (A,B) Viability of SKOV3 and HO8910 cells treated with ISO (0–20 µM) for 24 h measured by CCK-8 assay. (C,D) Effect of ISO 15 µM treatment for 1–5 days on the viability of OC cells determined by CCK-8 assay. SKOV3 and HO8910 cells were treated with 15 µM ISO for 24 h. (E) Colony formation assay. Crystal violet staining; magnification, ×1. (F,G) Wound healing experiment and images of monolayers were captured under an optical light microscope. Scale bar =200 µm. (H) Transwell assay. Crystal violet staining; scale bar =200 µm. (I) Western blot detects the expression of Ki67, MMP9 and MMP2 protein. Compared with the Control group, *, P<0.05. ISO, isorhamnetin; OC, ovarian cancer; MMP, matrix metalloproteinase; OD, optical density.

Page 8 of 13

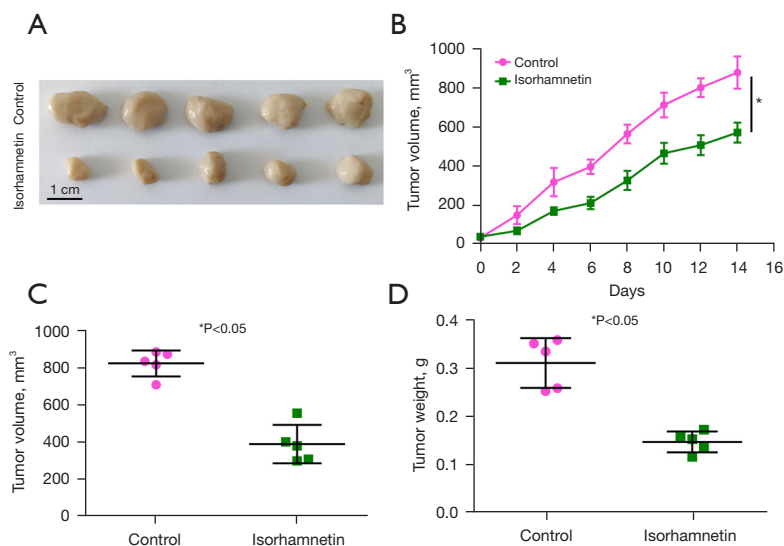Wang et al. Study on the anti-tumor effect of ISO in OC

Figure 4 ISO inhibits OC tumor growth *in vivo*. (A) Representative tumors from different groups of mice. (B) Monitoring of tumor volume at specified time points. Tumor volume (C) and tumor weight (D) were measured at the end of the experiment. Compared with the Control group, *, P<0.05. ISO, isorhamnetin; OC, ovarian cancer.

by western blotting. The protein level of ESR1 decreased with increasing ISO concentration (P<0.05, *Figure 6A*). At the same time, the protein level of ESR1 decreased with the passage of time after SKOV3 and HO8910 cells were treated with 15 μM ISO for 12, 24 and 48 h (P<0.05, *Figure 6B*). To further analyze whether ISO affects OC progression by regulating ESR1 expression, we transfected SKOV3 and HO8910 cells with ESR1 or 15 μM ISO alone and in combination for 24 h. The western blotting results showed that compared with the Control group, ESR1 protein expression was upregulated after ESR1 transfection, and downregulated in the ISO group. Compared with the ISO group, ESR1 protein expression was upregulated in the ESR1 + ISO group (P<0.05, *Figure 6C*). Subsequently, as shown in *Figure 6D-6I*, compared with the Control group, the viability of SKOV3 and HO8910 cells after ESR1 transfection was significantly increased, the numbers of colonies and invasive cells was significantly increased, and the width of the wound was significantly reduced (P<0.05), all of which was reversed after ISO treatment. Notably, ESR1 transfection significantly reversed the inhibitory effects of ISO on the proliferation, migration and invasion of SKOV3 and HO8910 cells (P<0.05). These results indicated that ISO inhibited the proliferation, migration and invasion of OC cells by regulating ESR1.

Discussion

In recent years, substantial evidence has shown that many natural product-based drugs have attracted the attention of scientists due to their beneficial effects on many diseases, especially tumor metastasis. ISO is an effective component of Chinese herbal medicine or Shenqi Fuzheng injection commonly used in clinical treatment of lung cancer, and with low side effects (16), but no confirmatory evidence for its effect on OC cells has been available to date. In the study of Chinese medicine compound preparations and monomers, network pharmacology has been widely used in China, including data collection, target prediction, multi-component interaction network analysis and signal pathway prediction. Network pharmacology emphasizes the integration of biological networks and drug action networks. It analyzes the relationship between the active components of drugs and disease-related genes through the nodes in the network. From finding a single component to comprehensive network analysis, it further clarifies the anticancer mechanism of each active component of drugs (17). We utilized a systems pharmacology method, target prediction, PPI analysis, biological process, and KEGG pathway analyses to explore the fundamental molecular mechanism of action of ISO its therapeutic effect
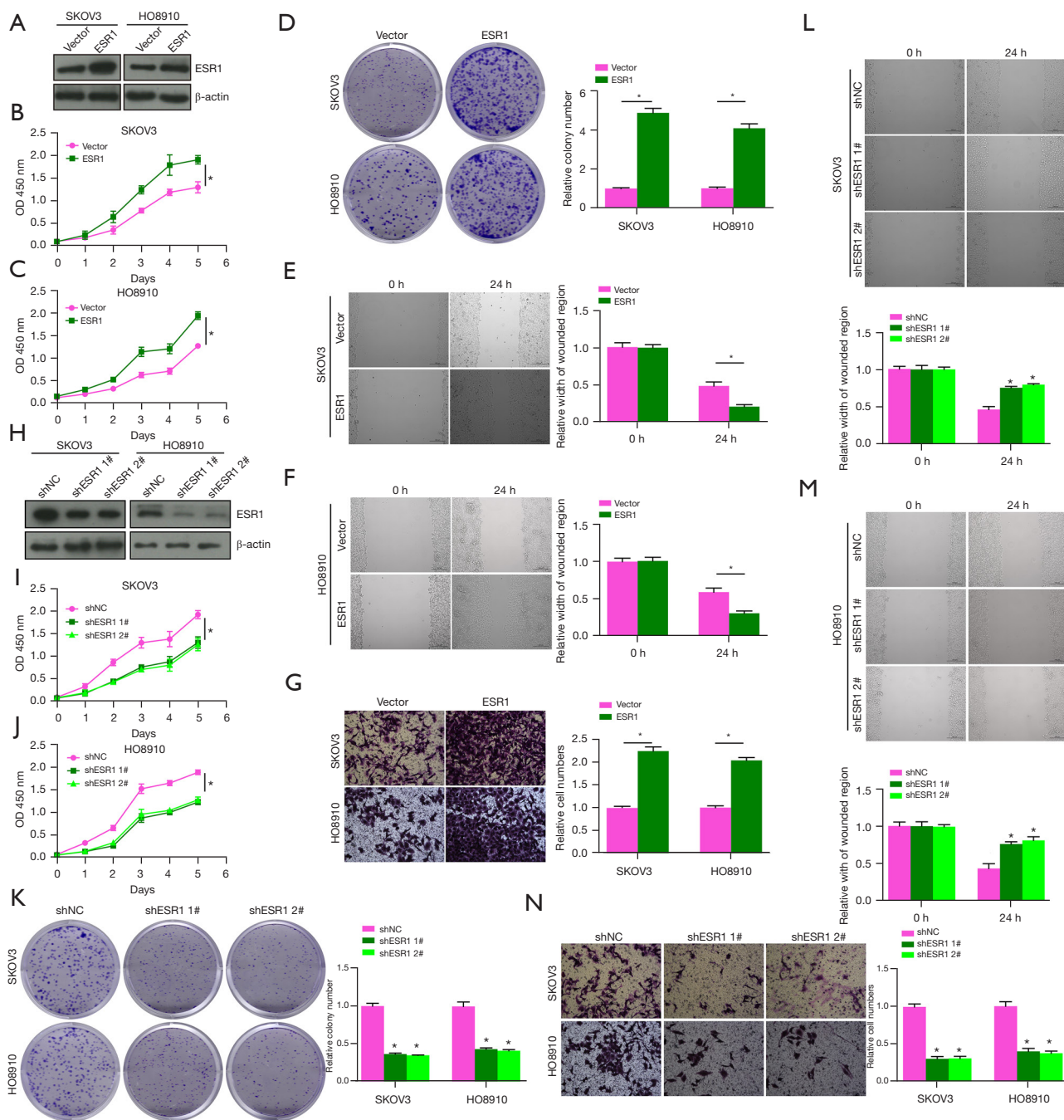
Figure 5 ESR1 promotes the proliferation, migration and invasion of OC cells *in vitro*. (A) ESR1 protein expression in SKOV3 and HO8910 cells after ESR1 overexpression. (B,C) SKOV3 and HO8910 cell viability after ESR1 overexpression. (D) SKOV3 and HO8910 cell colony formation. Crystal violet staining; magnification, ×1. (E,F) SKOV3 and O8910 wound healing and images of monolayers were captured under an optical light microscope. Scale bars =200 µm. (G) SKOV3 and HO8910 cell invasion. Crystal violet staining; scale bars =200 µm. (H) ESR1 protein expression in SKOV3 and HO8910 cells after knockdown of ESR1. (I,J) Cell viability after knockdown of ESR1. (K-M) SKOV3 and HO8910 cell colony formation (K; crystal violet staining; magnification, ×1) and wound healing (L,M; images of monolayers were captured optical light microscope, scale bars =200 µm). (N) SKOV3 and HO8910 cell invasion. Crystal violet staining; scale bars =200 µm. Compared with vector group or shNC group, *, P<0.05. OC, ovarian cancer; ESR1, estrogen receptor 1; OD, optical density; NC, negative control.

Page 10 of 13

Wang et al. Study on the anti-tumor effect of ISO in OC
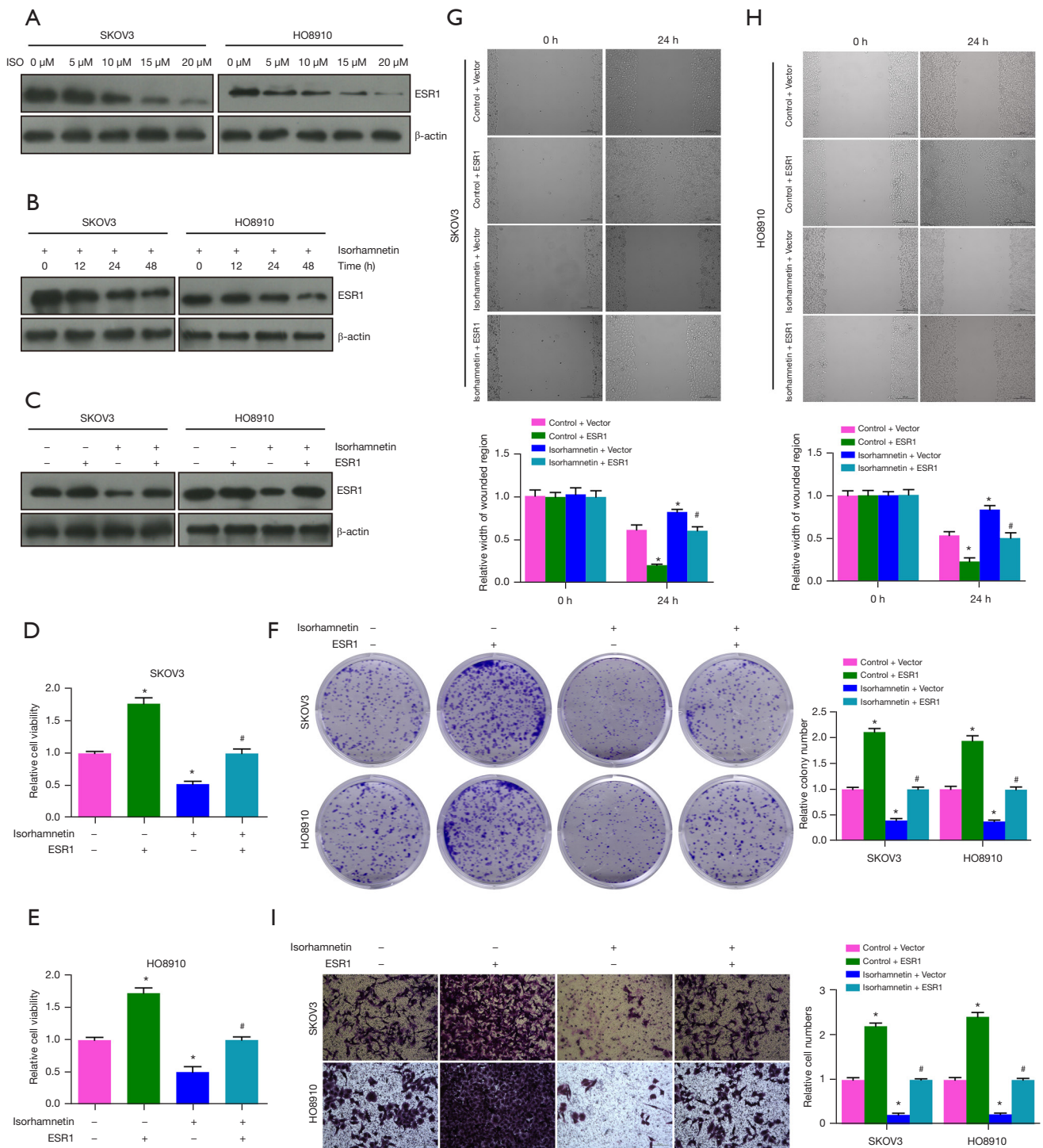

Figure 6 ISO inhibits proliferation, migration and invasion of OC cells by targeting ESR1. (A) ESR1 protein levels in SKOV3 and HO8910 cells treated with ISO (0–20 µM) for 24 h. (B) Protein levels of ESR1 in SKOV3 and HO8910 cells treated with 15 µM ISO for different lengths of time. (C) ESR1 protein levels in SKOV3 and HO8910 cells after ESR1 transfection and 15 µM ISO treatment alone or in combination. (D,E) Cell viability. (F) Colony formation. Crystal violet staining; magnification, ×1. (G,H) Wound healing and images of monolayers were captured under an optical light microscope. Scale bar =200 µm. (I) Cell invasion. Crystal violet staining; scale bar =200 µm. Compared with the Control group, *, P<0.05; compared with the ISO group, #, P<0.05. ISO, isorhamnetin; OC, ovarian cancer; ESR1, estrogen receptor 1.

in OC. First, we screened a total of 25 targets of ISO in treating OC. GO and KEGG pathway analyses showed that ISO regulated the proliferation, migration and apoptosis of OC cells, and may mediate a variety of cancer-related signaling pathways. PPI network analysis was performed on these targets to further explore the molecular mechanism of ISO in the treatment of OC. The upregulated genes in the GSE66957 database were then analyzed by the GEO2R website and intersected with the above 25 and target genes to obtain 13 overlapping genes. Further analysis of the expression and survival analysis of theses overlapping genes through the UALCAN database revealed that only the high expression of *ESR1* was associated with a decrease in the OS of OC patients. Therefore, we speculate that ESR1 may be a potential target of ISO in OC.

We then performed biological experiments to verify our analyses. CCK-8 and colony formation experiments showed that ISO could effectively inhibit the proliferation of SKOV3 and HO8910 cells in a concentration- and time-dependent manner. Through wound healing and wound healing experiments, we also found that ISO significantly inhibited the migration and invasion of SKOV3 and HO8910 cells. MMPs, including MMP2 and MMP9, are responsible for the degradation of the extracellular matrix and are associated with tumor growth, invasion and angiogenesis (4,18). Western blotting analysis showed that ISO significantly inhibited the expression of MMP2, MMP9 and Ki67, which suggested that ISO can effectively inhibit the adhesion, invasion and metastasis of OC cells. In this study, we observed that the tumor volume of the ISO group was significantly less than that of the Control group, and the tumor weight was significantly reduced, indicating that ISO significantly inhibited tumor growth *in vivo*.

The ovary is the main part of estrogen synthesis. During tumorigenesis, estrogen regulates the major physiological activities of the ovarian epithelium through its specific hormone receptor subtypes, including regulation of balance, proliferation, and abnormal differentiation (19). The ESR1 gene is localized in the nucleus and forms homodimers or heterodimers with ESR2 to regulate a variety of physiological processes (20). A large number of studies have shown that *ESR1* is associated with OC, breast cancer, endometrial cancer and other cancers (21-23). Sieh *et al.* (24) found that ESR1 is expressed in up to 60% of ovarian epithelial tumors, and its level is higher than that of normal ovaries. Recent studies have shown that *ESR1* expression is significantly increased in ovarian tissues and

promotes OC progression (19,25). High expression of estrogen receptor promotes the spread of lymph or blood vessels in high-grade serous OC, which is associated with poor clinical prognosis (26). Therefore, ESR1 may serve as a potential biomarker for risk stratification and regional metastasis in patients with OC. In order to study the role of *ESR1* in OC, the proliferation, migration and invasion of cell lines SKOV3 and HO8910 were observed after overexpression or knockdown of *ESR1*. Our results showed that overexpression of *ESR1* promoted the proliferation, migration and invasion of SKOV3 and HO8910 cells, whereas knockdown of *ESR*1 expression had the opposite effect. Consistent with previous studies (19,25), high *ESR1* expression promotes OC progression. As a target gene of ISO, we found that the protein expression level of ESR1 decreased with increasing ISO concentration and in a time-dependent manner. To further study whether ISO has a tumor suppressor role by inhibiting the expression of ESR1 in OC, SKOV3 and HO8910 cells were treated with 15 μM ISO and transfected with ESR1 for 24 h. We observed that transfection of ESR1 reversed the inhibitory effect of ISO on the proliferation, migration and invasion of OC cells, which indicated that ISO inhibited the development of OC by targeting *ESR1* expression.

Conclusions

We used network pharmacology and experimental models to predict and validate the antitumor effect of ISO in OC. ISO inhibits the proliferation, migration and invasion of OC cells *in vitro* and the growth of OC tumors *in vivo*. Mechanistically, the effect of ISO on OC progression is mediated by inhibiting the expression of the target gene *ESR1*. Our findings provide a theoretical basis for the application of ISO in clinical treatment.

Acknowledgments

Footnote

Reporting Checklist: The authors have completed the ARRIVE reporting checklist. Available at https://atm.amegroups.com/article/view/10.21037/atm-22-5064/rc

Data Sharing Statement: Available at https://atm.amegroups.

Page 12 of 13

Wang et al. Study on the anti-tumor effect of ISO in OC

com/article/view/10.21037/atm-22-5064/dss

Conflicts of Interest: All authors have completed the ICMJE uniform disclosure form (available at https://atm.amegroups.com/article/view/10.21037/atm-22-5064/coif). The authors have no conflicts of interest to declare.

Ethical Statement: The authors are accountable for all aspects of the work in ensuring that questions related to the accuracy or integrity of any part of the work are appropriately investigated and resolved. Animal experiments were performed under a project license (No. 20221014004) granted by ethics committee of West China Hospital of Sichuan University, in compliance with national guidelines for the care and use of animals.

Open Access Statement: This is an Open Access article distributed in accordance with the Creative Commons Attribution-NonCommercial-NoDerivs 4.0 International License (CC BY-NC-ND 4.0), which permits the non-commercial replication and distribution of the article with the strict proviso that no changes or edits are made and the original work is properly cited (including links to both the formal publication through the relevant DOI and the license). See: https://creativecommons.org/licenses/by-nc-nd/4.0/.

References

1. Qin C, Wu M, Wang X, et al. Study on the mechanism of Danshen-Guizhi drug pair in the treatment of ovarian cancer based on network pharmacology and in vitro experiment. PeerJ 2022;10:e13148.
2. Jin Z, Chenghao Y, Cheng P. Anticancer Effect of Tanshinones on Female Breast Cancer and Gynecological Cancer. Front Pharmacol 2021;12:824531.
3. Zhai T, Zhang X, Hei Z, et al. Isorhamnetin Inhibits Human Gallbladder Cancer Cell Proliferation and Metastasis via PI3K/AKT Signaling Pathway Inactivation. Front Pharmacol 2021;12:628621.
4. Luo W, Liu Q, Jiang N, et al. Isorhamnetin inhibited migration and invasion via suppression of Akt/ERK-mediated epithelial-to-mesenchymal transition (EMT) in A549 human non-small-cell lung cancer cells. Biosci Rep 2019;39:BSR20190159.
5. Xu Y, Tang C, Tan S, et al. Cardioprotective effect of isorhamnetin against myocardial ischemia reperfusion (I/R) injury in isolated rat heart through attenuation of apoptosis. J Cell Mol Med 2020;24:6253-62.
6. Hu J, Zhang Y, Jiang X, et al. ROS-mediated activation and mitochondrial translocation of CaMKII contributes to Drp1-dependent mitochondrial fission and apoptosis in triple-negative breast cancer cells by isorhamnetin and chloroquine. J Exp Clin Cancer Res 2019;38:225.
7. Qi F, Sun JH, Yan JQ, et al. Anti-inflammatory effects of isorhamnetin on LPS-stimulated human gingival fibroblasts by activating Nrf2 signaling pathway. Microb Pathog 2018;120:37-41.
8. Jaramillo S, Lopez S, Varela LM, et al. The flavonol isorhamnetin exhibits cytotoxic effects on human colon cancer cells. J Agric Food Chem 2010;58:10869-75.
9. Hu S, Huang L, Meng L, et al. Isorhamnetin inhibits cell proliferation and induces apoptosis in breast cancer via Akt and mitogen-activated protein kinase kinase signaling pathways. Mol Med Rep 2015;12:6745-51.
10. Ruan Y, Hu K, Chen H. Autophagy inhibition enhances isorhamnetin-induced mitochondria-dependent apoptosis in non-small cell lung cancer cells. Mol Med Rep 2015;12:5796-806.
11. Duan R, Liang X, Chai B, et al. Isorhamnetin Induces Melanoma Cell Apoptosis via the PI3K/Akt and NF-κB Pathways. Biomed Res Int 2020;2020:1057943.
12. Zhang R, Zhu X, Bai H, et al. Network Pharmacology Databases for Traditional Chinese Medicine: Review and Assessment. Front Pharmacol 2019;10:123.
13. Boezio B, Audouze K, Ducrot P, et al. Network-based Approaches in Pharmacology. Mol Inform 2017.
14. Li B, Jiang Y, Chu J, et al. Drug-Target Interaction Network Analysis of Gene-Phenotype Connectivity Maintained by Genistein. J Comput Biol 2020;27:1678-87.
15. Gu T, Yuan W, Li C, et al. α-Solanine Inhibits Proliferation, Invasion, and Migration, and Induces Apoptosis in Human Choriocarcinoma JEG-3 Cells In Vitro and In Vivo. Toxins (Basel) 2021;13:210.
16. Dong BY, Wang C, Tan L, et al. Inhibitory effect of Shenqi Fuzheng injection combined with docetaxel on lung cancer cells. J Zhejiang Univ Sci B 2017;18:76-8.
17. He R, Ou S, Chen S, et al. Network Pharmacology-Based Study on the Molecular Biological Mechanism of Action for Compound Kushen Injection in Anti-Cancer Effect. Med Sci Monit 2020;26:e918520.
18. Xie Q, Yang Z, Huang X, et al. Ilamycin C induces apoptosis and inhibits migration and invasion in triple-negative breast cancer by suppressing IL-6/STAT3 pathway. J Hematol Oncol 2019;12:60.
19. Li M, Shi M, Xu Y, et al. Histone Methyltransferase KMT2D Regulates H3K4 Methylation and is Involved

in the Pathogenesis of Ovarian Cancer. Cell Transplant 2021;30:9636897211027521.

20. Bao W, Zhang Y, Li S, et al. miR-107-5p promotes tumor proliferation and invasion by targeting estrogen receptor-α in endometrial carcinoma. Oncol Rep 2019;41:1575-85.

21. Gong G, Lin T, Yuan Y. Integrated analysis of gene expression and DNA methylation profiles in ovarian cancer. J Ovarian Res 2020;13:30.

22. Wang S, Li X, Zhang W, et al. Genome-Wide Investigation of Genes Regulated by ERα in Breast Cancer Cells. Molecules 2018;23:2543.

23. Wang Y, Lu Y, Li Z, et al. Oestrogen receptor α regulates the odonto/osteogenic differentiation of stem cells from apical papilla via ERK and JNK MAPK pathways. Cell Prolif 2018;51:e12485.

24. Sieh W, Köbel M, Longacre TA, et al. Hormone-receptor expression and ovarian cancer survival: an Ovarian Tumor Tissue Analysis consortium study. Lancet Oncol 2013;14:853-62.

25. Wang K, Zhu G, Bao S, et al. Long Non-Coding RNA LINC00511 Mediates the Effects of ESR1 on Proliferation and Invasion of Ovarian Cancer Through miR-424-5p and miR-370-5p. Cancer Manag Res 2019;11:10807-19.

26. Matsuo K, Sheridan TB, Mabuchi S, et al. Estrogen receptor expression and increased risk of lymphovascular space invasion in high-grade serous ovarian carcinoma. Gynecol Oncol 2014;133:473-9.

(English Language Editor: K. Brown)